

Thesis of Doctoral Dissertation

Tamás Dankó

Budapest

2021.



HUNGARIAN UNIVERSITY OF AGRICULTURE AND LIFE SCIENCES

Doctoral School of Horticultural Sciences

Transcriptome-level characterisation of the grape-*Botrytis* interaction during noble rot of the Furmint grape variety

Tamás Dankó

Budapest

2021.

Name of Ph.D. School: Doctoral School of Horticultural Sciences

Field: Crop Sciences and Horticulture

Head of Ph.D. School: *Zámboriné Dr. Éva Németh*

Doctor of the Hungarian Academy of Sciences

Head of Department of Medicinal and Aromatic
Plants

Hungarian University of Agriculture and Life
Sciences,
Faculty of Horticultural Science

Supervisors:

Dr. Horváthné Marietta Petróczy

Associate professor

Hungarian University of Agriculture and Life
Sciences

Department of Plant Pathology

Dr. Miklós Pogány

Senior research associate, PhD

Centre for Agricultural Research,
Plant Protection Institute

.....
Head of Ph.D. School

.....
Supervisor

.....
Supervisor

1. PREVIOUS RESEARCH AND MAIN OBJECTIVES

The „tokaji aszú” is one of the most unique wines in the world. In 2013 the government of Hungary selected “tokaji aszú” as a national value (Hungarikum). Noble rotted berries needed to make aszú wines are the result of a special interaction between ripe grapes and the fungus *Botrytis cinerea* Pers. If the weather is unfavourable for noble rot development, this sophisticated fungus-grape relationship might lead to gray mold symptoms instead. *B. cinerea* infections result in an estimated 10-100 billion dollars loss in the agricultural sector per year (Weiberg et al. 2013). Grapes are currently cultivated on nearly 7 million hectares worldwide (OIV-International Organisation of Vine and Wine). The fact that even complete crop losses can be caused by this fungal infection makes a comprehensive study of the grape - *B. cinerea* interaction particularly important.

At least four conditions must be simultaneously met to develop noble rot (Naár és Szarvas, 2012):

1. Wet weather at the beginning of noble rot, in order to develop a strong initial infection
2. Ripe or overripe grape berries
3. The epidermis of grape berries must be intact and unhurt
4. After the infection, weather should permanently remain dry and somewhat windy.

With these four conditions, the growth of the fungus is partly retarded.

Previously the grape-*Botrytis* interaction has been investigated by high throughput transcriptome analyses (Agudelo-Romero *et al.* 2015, Blanco-Ulate *et al.* 2015, Kelloniemi *et al.* 2015), but in these works noble rot and gray mold gene expression profiles have not been substantially compared.

In my work, I place special emphasis on the molecular biological comparison of the two different forms of the interaction, considering both the grape and fungal cells, which has not yet taken place in Hungarian Furmint samples.

Small RNAs are non-translated small RNA molecules, which can suppress the target gene mRNA expression. Small RNAs can modify the host's and also the pathogen's gene expression profile (Huang *et al.* 2019). Small RNA profile investigations have not been performed previously in the grape-*Botrytis* interaction.

The development of noble rot requires special climatic conditions, which are becoming less frequent in Tokaj-Hegyalja due to climate change. Modelling noble rot under growth chamber conditions therefore provides a highly prospective test environment. Grape volatiles significantly contribute to the aroma composition of wines. In the case of botrytized wines (such as tokaji aszú), the aromas of grape berries are supplemented with compounds from *B. cinerea*, which are formed during noble rot. Volatile profiles of noble rot and gray mold infections cannot be determined in the vineyard at the same time, due to the different weather conditions the two forms of the interaction require. By simulating noble rot and gray mold in climate chambers, it is possible to study the volatile profiles caused by the two forms of the infection under controlled conditions.

2. AIMS

1. Histopathological characterization of botrytized Furmint berries.
2. Total transcriptome analysis of Furmint berries in different noble rot stages.
Joint analysis of plant and fungal mRNA patterns.
3. Small RNA analysis of Furmint grape berries in consecutive noble rot stages.
Joint analysis of plant and fungal miRNA patterns.
4. Comparison of the total transcriptome results of Furmint under noble rot with other botrytized grape cultivars.
5. Modelling of noble rot in growth chambers using microclimatic parameters ideal for noble rot in the vineyard.
6. Determination of botrytized Furmint volatile markers.

3. MATERIALS AND METHODS

Noble rotted grape berries were collected in Mád, in the Tokaj wine region in 2016, 2017 and 2018. Four stages were determined based on morphological criteria:

- I. stage: Ripe, intact berries, tight skin with no visible fungal symptoms. The colour of the berries is greenish yellow.
- II. stage: Visible symptoms of *B. cinerea* infection. The peel of the berries is 25-90% brownish purple. The berry has lost its firmness.
- III. stage: The berry is completely brownish purple and slightly shrivelled.
- IV. stage: Finished, fully-shrivelled, raisin-like aszú berries with deep purple or brown colour.

3.1. Determination of fungal biomass

The fungal biomass was determined by *B. cinerea* specific ELISA kit (LOEWE) in different noble rot stages. Calibration curve was required to quantify the amount of the fungus, for which I used *B. cinerea* mycelia grown in liquid culture.

3.2. Berry vital staining

The basis for the determination of grape berry live tissues is based on a paper published by Fuentes et al. (2010). The cut surface of the halved berries was stained with Fluorescein diacetate fluorescein dye, thus making the living cells visible. Fluorescence signal was recorded under a fluorescence microscope equipped with a GFP filter. The image processing module of the MATLAB software was used for image analysis.

3.3. Total RNA and small RNA sequencing and data processing

Total RNA extraction was based on the work of Reid *et al.* (2010), small RNA extraction was based on the work of Carra *et al.* (2007).

The total transcriptome sequencing and subsequent data processing was performed by UD-GenoMed Ltd. (Debrecen). Sequencing was performed on a NextSeq500 (Illumina). Sequence alignment was performed using separate grape (*Vitis vinifera* IGGP 12x) (Jaillon *et al.* 2007) and *Botrytis cinerea* (ASM83294v1) (Van Kan *et al.* 2017) reference cDNA libraries. Raw expression values were normalized by the DESeq algorithm. List of differentially expressed genes was identified by Tukey post hoc and ANOVA tests combined with Benjamini-Hochberg false discovery rate (FDR) correction.

Small RNA sequencing was also performed on NextSeq500 (Illumina), similar to the total transcriptome sequencing. Reads were aligned to the *V. vinifera* reference genome. List of differentially expressed miRNAs between stages was identified by Tukey post hoc and ANOVA with Benjamini-Hochberg FDR correction. Target genes of miRNAs were predicted by PSRNATarget online server (Dai *et al.* 2018).

Validation of total transcriptome sequencing has been performed. The expression of 5 *V. vinifera* and 5 *B. cinerea* gene expression values were determined by Real-Time qPCR. The ddCt method was used to determine the change in expression.

GO overrepresentation tests were performed using Cytoscape Bingo. GO libraries of genes were created with Ensembl-Biomart and KEGG online servers. Hypergeometric statistics was used in the test and the results were corrected with Benjamini & Hochberg false discovery rate ($p < 0.01$, FDR).

3.4. Modelling of noble rot

Simulation of noble rot was carried out with freshly harvested, healthy, whole Furmint grape bunches. Bunches had been sprayed with 10^5 /ml *B. cinerea* conidium suspension and incubated overnight in closed boxes, before transferring them to a climate chamber. The adjusted climate parameters followed a daily cycle, that imitate vineyard conditions ideal for noble rot (Daytime 20 °C, RH%=60 and night 5-10 °C, RH%=98). After the overnight incubation in boxes

half of the bunches were placed on well-ventilated trays subjected to noble rot-inducing conditions and the other half were kept in closed humid boxes triggering gray mold.

3.5. Collection of infected grape volatiles

During the modelling of noble rot and gray mold in the climate chamber, dynamic volatile collection was carried out from infected bunches of grapes. Volatiles were trapped by active charcoal. Volatile compounds were quantified and identified by gas chromatograph linked mass-spectrometer (GC-MS).

4. RESULTS

4.1. Determination of fungal biomass

B. cinerea biomass was determined in noble rotted grape berries collected in 2016 and 2017. In the first year, whole grape berries were grinded and used. In the second year, distinct parts of the berries (seed, flesh, peel) were individually analysed. In both years, I found that the presence of the fungus was hardly detectable in the I. noble rot stage. The amount of *B. cinerea* increased considerably in stage II., and in stage III. it reached a maximum level. In stage IV. the biomass of *B. cinerea* got slightly reduced. At the beginning of noble rot *B. cinerea* could only be detected in the skin. In stage III. and IV. *B. cinerea* was detected mostly in the flesh of the berries.

4.2. Results of berry vital staining

In 2017 the proportions of living cells was determined in each stages of noble rot in Furmint berries. During the assay, the FDA dye enters the cells, where it is converted into a fluorophore compound by non-specific esterases. Fluorescence was detected using a fluorescence microscope and the images were analysed using Matlab software. Due to the different berry sizes, it was necessary to normalize the data, which I achieved by determining the perimeter of the berry. In the second stage, the amount of living tissue is 36% compared to stage I., and in the third stage it is only 4%. In stage IV. no fluorescent signal could be detected.

4.3. Results of total transcriptome sequencing in Furmint during noble rot

In grape and *B. cinerea* data analyses of total transcriptome sequencing the expression values were compared to stage I. Grape sequencing results obtained in stage IV. derive from the seeds (see 3.2. chapter), so I did not take them into account in the analysis of biological processes. The gene expression profiles obtained from sequencing show characteristic patterns between stages in grape cells (Fig. 1), as well as in fungal cells, but similar patterns can be observed in samples belonging to the same stage.

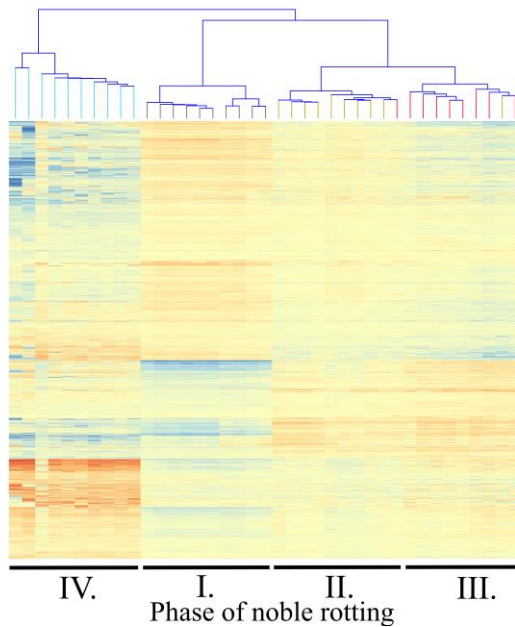


Figure 1.

Expression values of total transcriptome analysis of Furmint during noble rot. Hierarchical clustering results are shown.

1637 induced genes were identified in the I. noble rot stage and 2126 genes in stage II. The overlap was high – 1517 induced genes were the same in both stages. GO overrepresentation test was performed to evaluate biological processes. Genes responsible for defence, chitin metabolism, cell wall modification and redox processes were induced in both stages.

4.4. Activation of grape antioxidant systems during noble rot

Two genes of the identified 17 *glutathione peroxidase* genes and 18 *glutathione s-transferase* genes were induced in Furmint during noble rot. Two *superoxide dismutase* (SOD) genes were also induced, and the expression of two *catalase* genes was decreased. Sixteen genes of the identified 90 *peroxidase* genes were induced in the II. and 15 genes in the III. noble rot stage.

4.5. Synthesis of secondary metabolites from degradation of L-phenylalanine

Metabolism of L-phenylalanine in plant cells produces phenylpropanoid, stilbene and flavonoid precursors. The expression of ten *phenylalanine-ammonia-lyase* genes increased by 1-3 (log2) during noble rot. The expression of *trans-cinnamic acid-4-monooxygenase* was greatly increased and the expression of *4-coumaryl-Coa ligase* genes was also increased in both stages. These genes are necessary in the consecutive steps of phenylpropanoid biosynthesis.

The *p-coumaryl-3-hydroxylase* genes were not induced, therefore the pathway of lignin biosynthesis was inactive. In contrast, *stilbene-synthase* genes were induced in large numbers. *UDP-Glc: flavonoid 3-O-glycosyltransferase (UF3GT)* is responsible for the final glycosylation in the synthesis of anthocyanins. Transcription of several *UF3GT* genes was increased during noble rot of Furmint. Three *UF3GT* genes, located in the same cluster in the genome are induced exclusively during noble rot (Agudelo-Romero *et al.* 2015, Blanco-Ulate *et al.* 2015, Kelloniemi *et al.* 2015).

4.6. PR genes in the process of Furmint noble rot

The fundamental salicylic acid-mediated signalling pathway induces *PR1* (*Pathogenesis-related*), *PR2* and *PR5* genes. These groups of *PR* genes are mainly repressed during noble rot of Furmint. The jasmonic acid mediated signalling pathway induces *PR3*, *PR4* and *PR12* genes, and these groups were induced during Furmint noble rot. Notable induction was observed in group *PR6*, where all genes were strongly induced.

4.7. Transcription factors in the process of noble rot in Furmint

Six transcription factor (TF) families (*AP2/ERF*, *bHLH*, *MYB*, *NAC*, *WRKY*, *bZIP*) are responsible for plant defence against pathogens. Expression of 23 *AP2/ERF* TF genes was increased in Furmint samples. Expression of 11 of the 115 identified *bHLH*-type TF genes was also altered. Half of them were induced.

Expression of 14 *MYB* TF genes was altered significantly as well, and third of them were repressed. Nine of the 11 altered *NAC* TF genes were induced. Expression of 11 *bZIP*-type TF genes (out of 47) was altered. Twenty-three *WRKY* TF genes were identified in grapevine, and almost half of them were induced in the second stage of noble rot.

4.8. Comparison of transcriptional profiles of Furmint and Semillon varieties during noble rot

The profiles of induced genes in the II. and III. noble rot stages of Furmint (Tokaj, Hungary) and Semillon (California, USA) were compared. 1186 induced genes in the second stage and 1430 in the third stage were identical in the two stages. These comprised almost half of the whole altered gene set.

The profiles of transcription factors of Furmint and Semillon II. stage samples were compared. All six examined *TF* genes had similar rates of induced and repressed TFs within a particular TF family. In many cases, the expression values of the same genes were altered, thus forming similar TF profiles.

The number of differentially expressed *PR* genes was compared during noble rot of Furmint and Semillon grape varieties. Forty-six vs. 71 differentially expressed *PR* genes were detected in Furmint and in Semillon, respectively. Only jasmonic acid mediated *PR* genes (*PR3*, *PR4*, *PR12*) were induced in Furmint. However, both the jasmonic acid mediated and the salicylic acid (*PR1*, *PR5*) mediated genes were induced in the Semillon variety. Genes of the *PR6* group were also strongly induced in both cases.

4.9. Comparison of the transcriptional profiles between noble rot and gray mold

The total transcriptome profiles of noble rot (Furmint, stage II.) and gray mold (Marselan) samples (Kelloniemi *et al.* 2015) were compared. Slightly more than

600 genes (22% of genes with altered expression) were identical in the two infection forms. Comparing the expression values of *TF* encoding genes, less *TF* genes are induced in grapes during gray mold. Mainly increased expression of *AP2/ERF*, *MYB* and *WRKY* TF genes were lacking in gray mold, while these *TF* encoding genes were strongly induced in noble rot.

The number of differentially expressed *PR* genes were also compared in noble rot and gray mold. The number of *PR* genes with altered expression was almost the same (noble rot: 46, grey mold: 49). Ninety percent of differentially expressed *PR* genes in gray mold were induced, while in noble rot only 70%. Only jasmonic acid mediated *PR* genes (*PR3*, *PR4*, *PR12*) were induced in Furmint berries exposed to noble rot. However, in gray mold the jasmonic acid mediated and also the salicylic acid (*PR1*, *PR5*) mediated *PR* genes were induced.

Antioxidant systems were compared between noble rot of Furmint and gray mold of cultivar Marselan. Some *SOD* and *catalase* genes were induced in gray mold, similar to noble rot. *Glutathione-peroxidase* genes were induced neither in noble rot nor in gray mold. The most important difference here was the expression profile of *glutathione-s-transferase (GST)* genes. While 18 *GST* transcripts were strongly induced in Furmint, in Marselan only 4 *GST* genes were induced.

4.10. Results of *B. cinerea* total transcriptome sequencing

The transcriptome sequencing results of *B. cinerea* yielded valid results in all four stages of noble rot, because living fungal cells are present even in the dead stage IV. berries. Based on the results of the GO enrichment analysis, transport processes are most activated. Fewer transport processes are activated in stage II. compared to stage III. and they typically represent transport mechanisms of amino acids and polymers. In contrast, a remarkable increase in carbohydrate, peptide, and cofactor transport processes appears in stage III.

A large set of genes (275) encoding enzymes that are involved in extracellular carbohydrate metabolism was identified in *B. cinerea* previously (Blanco-Ulate

et al. 2014). Expression of these genes was analysed in our Furmint samples. *Endo-polygalacturonase-1* and *endo-polygalacturonase-2* genes were induced at an early stage of noble rot, similar to *pectin-methyltransferase*, *pectin-lyase* and *pectate-lyase* genes. Expression level of *endo-polygalacturonase-6* on the other hand was increased only later, similar to *endo-rhamnogalacturonase*, *endo- β -glucanase* and *rhamnogalacturonase* genes.

Expression level of *B. cinerea* genes that encode various components of the antioxidant system were also investigated. *SOD* genes were not induced in the fungus in our noble rot samples, however three *catalase*, three *peroxidase* and nine *glutathione-s-transferase* genes were upregulated.

Forty-four key enzymes are responsible for the biosynthesis of secondary metabolites in *B. cinerea* (Collado 2015). Sixteen of those genes exhibited altered expression level in our samples. *Polyketide synthase-6* for example, which is responsible for a key step in the biosynthesis of botcinic acid (Dalmais *et al.* 2011) was transcriptionally induced at an early stage of noble rot.

4.11. Results of small RNA sequencing

Twenty-one differentially expressed *V. vinifera* miRNAs were identified in noble rotted samples. Nine out of 15 in stage II., and 19 out of 34 identified miRNAs were induced in stage III. Targets of miRNAs were an *RNA biogenesis-related* gene, a presumed *NB-LRR* gene and a *HD-ZIP* TF gene in stage II. Gene expression levels of these target genes decreased 1.7-2.5 times in stage II. Expression of one miRNA was repressed in stage II., and its target gene's expression level was increased accordingly.

In stage III of noble rot targets of miRNAs were an *RNA biogenesis-related* gene, a presumed *NB-LRR* gene, three TF genes of *GRAS*, two TFs of *HD-ZIP*, two of *SBP* TF family, and one *MYB* TF gene. miRNAs are typically responsible for silencing a whole TF family, such as *VvmiR171b* and *VvmiR171i* for the *GRAS*, *VvmiR166a* for the *HD-Zip*, *VvmiR156b* for the *SBP*, and *VvmiR159c* for the *MYB*

TF family. As a result of gene silencing, expression levels of these target genes were decreased 1.6-4.7 times in comparison with the control samples. *V. vinifera* miRNAs were also aligned to the *B. cinerea* genome to reveal potential plant-fungus gene silencing interactions. Only one *B. cinerea* chaperon gene was targeted by grape miRNAs in stage II, and an additional two in stage III.

4.12. Volatile collections from bunches subjected to noble rot or gray mold development

Volatile collections were performed from the headspace of botrytized grape bunches incubated in airtight polyester bags. Thirty-five peaks were quantified and 32 compounds were identified. Volatile profiles of noble rot and gray mold samples were similar. Aliphatic alcohols, carboxylic acid derivatives, monoterpenes and aromatic molecules appeared in both infection forms. Nine compounds were emitted in significantly different concentration between gray mold and noble rot. Quantity of phenethyl alcohol, [S,S]-2,3-butanediol, acetic acid, 1-octen-3-ol, acetoin, isoamyl alcohol and isobutanol were increased in gray mold. Formation of trans-geranylacetone and sulcatone increased in the one-week-old noble rotted samples.

5. CONCLUSIONS

In my Ph.D. dissertation I present results on the molecular details of the *Vitis vinifera*-*Botrytis cinerea* interaction during noble rot in Tokaj-Hegyalja (Hungary). My research covers some macroscopic studies, plant and fungal total transcriptome analyses, small RNA analyses and volatile profile determination.

The distribution of *Botrytis cinerea* was determined by ELISA technique in noble rot berries. In mature, healthy berries (stage I. of noble rot) *B. cinerea* can be detected only on the berry surface, but in subsequent noble rot stages the fungal biomass is gradually increasing inside the berry. The highest biomass amount of *B. cinerea* was detected in the third stage of noble rot, then the concentration of fungal biomass decreased for the last stage.

I have adapted a semi-automatized living tissue detection system, which is able to determine the vitality of fruit tissues. This method is based on fluorescein-diacetate stain, which emits green light when exposed to UV light in living cells. The fluorescent green light was detected by high sensitivity full frame camera, then images were analysed by an algorithm that I had developed. A great percentage of grapevine berry cells died already in stage II. In stage III. living cells could be detected only around the seeds. These findings are consistent with our mRNA sequencing results, where the ratio of mapped reads that could be aligned with the *V. vinifera* reference cDNA database declined drastically in the successive stages of noble rot.

The results of transcriptome sequencing revealed that similar biological processes were induced in stage II. and III. noble rot berries. Genes encoding cell wall modifying enzymes, antioxidant systems (GSTs, peroxidases), heat shock proteins, PR proteins, response to biotic stress transcription factors and enzymes of the phenylpropanoid pathway were strongly induced during noble rot. The gene expression pattern of Furmint berries subjected to noble rot was highly similar to

the expression pattern of other grapevine varieties undergoing noble rot. This observation leads to the conclusion, that noble rot is a common biological process, which is not strictly cultivar-dependent. Nevertheless, Furmint also showed some genotype-specific molecular processes, such as the activation of *JAZ* genes, the induction of genes encoding *bHLH* TFs or the exclusive activation of JA-induced *PR3*, *4* and *12* genes within the group of genes encoding Pathogenesis-Related proteins.

Characteristic gene expression patterns of noble rot were successfully identified in comparison with gray mold or immature grape berry infection. These marker processes comprised the increased transcript level of GST and peroxidase isoforms, which are mostly lacking in berries affected by gray mold. The transcript levels of *AP2/ERF* TFs (which provide tolerance to biotic and abiotic stress) are significantly increased during noble rot. This process might be connected to osmotic stress due to the shrivelling of berries.

The *VIT_08s0058g01390* gene is a *V. vinifera*-specific WRKY TF, which has the highest expression value among the WRKY TFs in the Tokaj-Hegyalja samples. This gene is a noble rot-specific WRKY TF. The expression of *VvMYB14* and *VvMYB15* TF genes were also increased during noble rot. These TFs possess a regulatory role in the activity of *stilbene synthase* genes, therefore the transcription of *stilbene synthase* genes is more pronounced in noble rot berries than in gray mold berries.

The *VvUF3GT* genes have a key role in anthocyanin biosynthesis, but these genes are typically not transcribed in healthy white grape berries. Strikingly, as a result of noble rot induction *VvUF3GT* genes are strongly expressed in Furmint, contributing to the brownish purple colour of noble rotted Furmint berries. Considering results of the transcriptome study and the modeling of noble rot development in growth chambers, we can conclude that the key factor deciding about the outcome of the infection is the weather.

If the weather is warm and dry following the onset of the fungal infection, the growth of *B. cinerea* slows down. In this case, grape berries are able to initiate some defence processes (biosynthesis of stilbenes, cell wall modification, activation of the redox system), which further restrict the growth of the fungus and noble rot develops.

If rainy, humid weather sustains after the beginning of the infection, then gray mold develops, because the plant is running out of time to induce defence responses.

This research is the first example of small RNA sequencing of grape berries enduring noble rot. Grapevine small RNAs suppress plant development and cell growth in the berries at an early stage of noble rot. At a later stage this suppression of development and cell growth is even more pronounced, and TFs become the main small RNA targets.

Concerning the transcription of *Botrytis cinerea*, less *cutinase*, *catalase*, *secondary metabolite* and *peroxidase* genes are induced in the fungus during noble rot than in gray mould. Despite these differences, the gene expression profiles of the fungus in noble rot and gray mold are similar, suggesting that the outcome of the infection is not highly dependent on the metabolism of the fungus.

I simulated the process of gray mold and noble rot in a climate chamber simultaneously, mimicking a prolonged rainy period, which favors gray mold and a cycle of consecutive dry and humid periods, supporting noble development. Volatile compounds were collected from the air space of the resulting gray mold and noble rot clusters, and then these volatiles were identified and quantified. As botrytization progresses, the volatile emission of bunches changes. The volatile profile of gray mold is similar to that of noble rot, however, the amount of some alcohols, mainly from fermentation, increases dramatically.

I present my results here, retrieved from a detailed molecular study of noble rot that takes place in the Tokaj vine region of Hungary. A set of marker genes and gene groups that are specific for noble rot of Furmint are revealed.

6. NEW SCIENTIFIC RESULTS

- 1) Cells of Furmint berries die at an early stage of noble rot.
- 2) The transcriptional profiles of the grapevine cultivar Furmint and the filamentous fungus *Botrytis cinerea* were constructed during the process of noble rot.
- 3) The transcription of *glutathione S-transferase* genes and genes involved in the phenylpropanoid metabolism (*VvMyb14*, *VvMyb15*, *VvMybPA1*, *VvMybC2-L1*, *VvUF3GT*) are markedly different between noble rot of Furmint and gray mold.
- 4) Activation of *cutinase* genes does not occur in *B. cinerea* cells during noble rot, but *cutinase* genes (*Bcin01g10830*, *Bcin01g09430*, *Bcin07g01240*) are induced in gray mold.
- 5) I constructed the small RNA profile of Furmint berries subjected to noble rot and predicted the target genes in both the grapevine and the *B. cinerea* genomes.
- 6) Several volatile markers of gray mold and noble rot were defined for the Furmint grapevine variety. Gray mold can be associated with an increased formation of acetic acid, isoamyl alcohol, phenethyl alcohol, and 1-octen-3-ol, while berries exposed to noble rot produce more trans-geranylacetone and sulcatone.

7. LITERATURE

1. Agudelo-Romero P., Erban A., Rego C., Carbonell-Bejerano P., Nascimento T., Sousa L., Martínez-Zapater M., J., Kopka J., Fortes M., A. (2015) Transcriptome and metabolome reprogramming in *Vitis vinifera* cv. Trincadeira berries upon infection with *Botrytis cinerea*. *Journal of Experimental Botany* 66(7):1769–1785.
2. Blanco-Ulate B., Amrine K.C., Collins T.S., Rivero M. R., Vicente R. A., Morales-Cruz A., Doyle I. C., Ye Z., Allen G., Heymann H., Ebeler E. S., Cantu D. (2015) Developmental and Metabolic Plasticity of White-Skinned Grape Berries in Response to *Botrytis cinerea* during Noble Rot. *Plant Physiology* 169(4):2422-2443
3. Blanco-Ulate B., Morales-Cruz A., Amrine K.C., Labavitch J.M., Powell A.L., Cantu D. (2014) Genome-wide transcriptional profiling of *B. cinerea* genes targeting plant cell walls during infections of different hosts. *Frontiers in Plant Science* 5:435
4. Carra A., Gambino G., Schubert A. (2007) A cetyltrimethylammonium bromide-based method to extract low-molecular-weight RNA from polysaccharide-rich plant tissues. *Analytical Biochemistry* 360(2):318–20
5. Collado I.G., Viaud M. (2015) Secondary metabolism in *Botrytis cinerea*: Combining genomic and metabolomic approach 296-302 p. In: Fillinger S., Elad Y. (Szerk) *Botrytis – the fungus, the pathogen and its management in agricultural systems* Svájc Springer International kiadó 486
6. Dai X., Zhuang Z., Zhao P.X. (2018) psRNATarget: a plant small RNA target analysis server. *Nucleic Acids Research* 46(W1):W49–W54
7. Dalmais B., Schumacher J., Moraga J., LE Pêcheur P., Tudzynski B., Collado I.G., Viaud M. (2011) The *Botrytis cinerea* phytotoxin botcinic acid requires two polyketide synthases for production and has a redundant role in virulence with botrydial. *Molecular Plant Pathology* 12(6):564–79
8. Fuentes S., Sullivan W., Tilbrook J., Tyerman S. (2010) A novel analysis of grapevine berry tissue demonstrates a variety-dependent correlation between tissue vitality and berry shrivel. *Australian Journal of Grape and Wine Research* 16(2):327–336
9. Jaillon O., Aury J.M., Noel B., Clepet C., Casagrande A., Choisne N., Aubourg S., Vitulo N., Jubin C., Vezzi A., Legeai F., Huguency P., Dasilva C., Horner D., Mica E., Jublot D., Poulain J., Bruyère C., Billault A., Segurens B., Gouyvenoux M., Ugarte E., Cattonaro F., Anthouard V., Vico V., Del Fabbro C., Alaux M., Di Gaspero G., Dumas V., Felice N., Paillard

- S., Juman I., Moroldo M., Scalabrin S., Canaguier A., Le Clainche I., Malacrida G., Durand E., Pesole G., Laucou V., Chatelet P., Merdinoglu D., Delledonne M., Pezzotti M., Lecharny A., Scarpelli C., Artiguenave F., Pè M.E., Valle G., Morgante M., Caboche M., Adam-Blondon A.F., Weissenbach J., Quétier F., Wincker P; French-Italian Public Consortium for Grapevine Genome Characterization. (2007) The grapevine genome sequence suggests ancestral hexaploidization in major angiosperm phyla. *Nature* 449(7161):463-467
10. Kelloniemi J., Trouvelot S., Héloir M.C., Simon A., Dalmais B., Frettinger P., Cimerman A., Fermaud M., Roudet J., Baulande S., Bruel C., Choquer M., Couvelard L., Duthieuw M., Ferrarini A., Flors V., Le Pêcheur P., Loisel E., Morgant G., Poussereau N., Pradier J.M., Rascle C., Trdá L., Poinssot B., Viaud M. (2015) Analysis of the molecular dialogue between gray mold (*Botrytis cinerea*) and grapevine (*Vitis vinifera*) reveals a clear shift in defense mechanisms during berry ripening. *Molecular Plant–Microbe Interactions* 28(11):1167–1180
 11. Naár Z., Szarvas J. (2012) Borászati Mikrobiológia. Eger: Eszterházy Károly Főiskola nyomda, 196 p.
 12. Huang C.Y., Wang H., Hu P., Hamby R., Jin H. (2019) Small RNAs - Big Players in Plant-Microbe Interactions. *Cell Host & Microbe* 26(2):173-182.
 13. Reid K.E., Olsson N., Schlosser J., Peng F., Lund S.T. (2006) An optimized grapevine RNA isolation procedure and statistical determination of reference genes for real-time RT-PCR during berry development. *BMC Plant Biology* 6:27
 14. van Kan J.A., Stassen J.H., Mosbach A., Faino L., Farmer A.D., Papanastasiou D.G., Zhou S., Seidl M.F., Cottam E., Edel D., Hahn M., Schwartz D.C., Dietrich R.A., Widdison S., Scalliet G. (2017) A gapless genome sequence of the fungus *Botrytis cinerea*. *Molecular Plant Pathology* 18(1):75-89
 15. Weiberg A., Wang M., Lin F.M., Zhao H., Thang Z., Kaloshian I., Huang H., Jin H. (2013) Fungal small RNAs suppress plant immunity by hijacking host RNA interference pathways. *Science* 342(6154):118-123

8. SCIENTIFIC PUBLICATIONS

Papers in journals with impact factors

Dankó T., Szelényi M., Janda T., Molnár B.P., Pogány M. (2021) Distinct volatile signatures of bunch rot and noble rot, *Physiological and Molecular Plant Pathology*, *accepted*

Balogh E., Juhász Cs., **Dankó T.**, Fodor J., Tóbiás I., Gullner G. (2020) The expression of several pepper fatty acid desaturase genes is robustly activated in an incompatible pepper-tobamovirus interaction, but only weakly in a compatible interaction, *Plant Physiology and Biochemistry* 148:347-358. IF: 3,7

Kámán-Tóth E., **Dankó T.**, Gullner G., Bozsó Z., Palkovics L., Pogány M. (2018) Contribution of cell wall peroxidase- and NADPH oxidase -derived reactive oxygen species to *Alternaria brassicicola* -induced oxidative burst in *Arabidopsis*, *Molecular Plant Pathology* 20(4):485-499. IF.: 4,18

Kámán-Tóth E., Pogány M, **Dankó T.**, Szatmári Á., Bozsó Z. (2018) A simplified and efficient *Agrobacterium tumefaciens* electroporation method, *3Biotech* 8:148 IF.: 1,36

Fodor J., Kámán-Toth E., **Dankó T.**, Schwarczinger I., Bozsó Z., Pogány M. (2018) Description of the *Nicotiana benthamiana*-*Cercospora nicotianae* Pathosystem, *PHYTOPATHOLOGY* 108(1):149-155. IF: 2,9

Fodor J., Köblös G., Kákai Á., Kárpáti Zs., Molnár B.P., **Dankó T.**, Bozsik G., Bognár Cs., Szöcs G., Fónagy A. (2017) Molecular cloning, mRNA expression and biological activity of the pheromone biosynthesis activating neuropeptide (PBAN) from the European corn borer, *Ostrinia nubilalis*, *Insect Molecular Biology* 26(5):616-632. IF.: 2,9

Pogány M., **Dankó T.**, Kámán-Tóth E., Schwarczinger I., Bozsó Z. (2015) Regulatory Proteolysis in *Arabidopsis*-Pathogen Interactions, *International Journal of Molecular Science* 16(10): 23177-23194. IF.: 3,2

Köblös G.¹, **Dankó T.**¹, Sipos K., Geigner Á., Fodor J., Fónagy A. (2014) The Regulation of *Δ11-desaturase* gene expression in the pheromone gland of *Mamestra brassicae* (Lepidoptera; Noctuidae) during pheromonogenesis, *General and Comparative Endocrinology* 221:217-227. IF.: 2,4

Papers in journals without impact factors

Oláh Cs., Nagy T., **Dankó T.**, Petróczy M., Pogány M. (2019) A *Botrytis cinerea* látens fertőzése Tokaj-hegyalján *Növényvédelem* 80(55):101-109.

Balogh E., Juhász Cs., **Dankó T.**, Fodor J., Tóbiás I., Gullner G. (2019) A zsírsav-deszaturáz gének aktiválódása paprika levelekben tobamovírus fertőzések hatására *Növényvédelem* 80(55):443-453.

Dankó T., Kámán-Tóth E., Petróczy M., Pogány M. (2017) Abiotikus paraméterek hatása a *Botrytis cinerea* produkció biológiájára *Növényvédelem* 78(11): 497-506.

Conference proceedings

Dankó T., Kámán-Tóth E., Vági P., Pogány M. (2018) Grape berry and *Botrytis cinerea* parameters during noble rot of Tokaj's grape samples, Denmark, Copenhagen: Plant biology Europe ISBN: 978-87-996274-1-7 pp. 193

Dankó T., Kámán-Tóth E., Vági P., Pogány M. (2018) Description of grape berry (cultivar Furmint) and *Botrytis cinerea* parameters in the process of botrytization, Budapest, Magyarország, Fialat Biotechnológusok Országos Konferenciája

Dankó T., Kámán-Tóth E., Vági P., Gellért Á., Bozsó Z., Pogány M. (2017) Az *Arabidopsis AT4G10540* szubtiláz befolyásolja a növény kórokozókkal szembeni válaszát, Budapest, Magyarország: Magyar Növényvédelmi Társaság, ISSN: 0231 2956 pp. 91

Köblös G., **Dankó T.**, Sipos K., Geigner Á., Fodor J., Fónagy A. (2014) The Regulation of *Δ11-desaturase* gene expression in the pheromone gland of *Mamestra brassicae* (Lepidoptera; Noctuidae) during pheromonogenesis, Renne, Franciaország: *The 27th Conference of European Comparative Endocrinologists*, VIII. pp. 25-29